Osteoarthritis and Cartilage 22 (2014) 95–103

Osteoarthritis and Cartilage

A numerical model to study mechanically induced initiation and progression of damage in articular cartilage

S.M. Hosseini, W. Wilson, K. Ito, C.C. van Donkelaar*

Department of Biomedical Engineering, Gem-Z 4.101, Eindhoven University of Technology, PO Box 513, 5600 MB Eindhoven, The Netherlands

ARTICLE INFO

Article history:
Received 31 May 2013
Accepted 23 October 2013

Keywords:
Osteoarthritis
Damage mechanics
Cartilage softening
Collagen damage

SUMMARY

Objective: Proteoglycan (PG) loss and surface roughening, early signs of osteoarthritis (OA), are likely preceded by softening of the ground substance and the collagen network. Insight in their relative importance to progression of OA may assist the development of treatment strategies for early OA. To support interpretation of experimental data, a numerical model is proposed that can predict damage progression in cartilage over time, as a consequence of excessive mechanical loading. The objective is to assess the interaction between ground substance softening and collagen fiber damage using this model.
Design: An established cartilage mechanics model is extended with the assumption that excessive strains may damage the ground substance or the collagen network, resulting in softening of the overstrained constituent. During subsequent loading cycles the strain may or may not cross a threshold, resulting in damage to stabilize or to progress. To evaluate how softening of the ground substance and collagen may interact, damage progression is computed when either one of them, or both together are allowed to occur during stepwise increased loading.
Results: Softening in the ground substance was predicted to localize in the superficial and transitional zone and resulted in cartilage softening. Collagen damage was most prominent in the superficial zone, with more diffuse damage penetrating deeper into the tissue, resulting in adverse strain gradients. Effects were more pronounced if both constituents developed damage in parallel.
Conclusion: Ground substance softening and collagen damage have distinct effects on cartilage mechanopathology, and damage in either one of them may promote each other.
© 2013 Osteoarthritis Research Society International. Published by Elsevier Ltd. All rights reserved.

Introduction

Articular cartilage derives this biomechanical function from the constitution of its extracellular matrix (ECM), which consists of a strongly hydrated ground substance, mainly consisting of proteoglycans (PGs), reinforced by a tension-resistant fibrillar collagen network. The PGs attract water through osmotic pressure, therewith resisting compression and straining the collagen. Unfortunately, this load bearing construction may become damaged when cartilage is subjected to excessive mechanical conditions, and such damage is likely to progress into osteoarthritis (OA)[1–4]. Early signs of OA include PG loss and cartilage surface roughening, which proceed into fibrillation with cracks penetrating deeper into the tissue at later stages[5–9]. It is apparent that these changes reduce tissue stiffness under tension[8,10,11], compression and shear, and increase permeability[12]. It has become apparent that initial damage may start before PGs are lost and the surface roughens. As a consequence of loading with an indenter, collagen damage was detected below the cartilage surface, but it did not necessarily become apparent at the surface[13]. Similar loading conditions were later associated with cartilage softening[14]. These effects may corroborate with observations of damage to the collagen fiber structure at the microscopic scale in early OA tissue[5,15,16]. However, softening also occurred without detectible collagen damage or loss of PGs from the tissue. Therefore, it was proposed that softening may result from damage to the PG-rich ground substance[14], or from the interaction between PGs and collagen at the microscopic scale[17,18].

Because together they determine the mechanical properties of articular cartilage, softening or either the ground substance or the collagen network may affect the strains experienced by the other. However, the importance of such interaction to the progression of

* Address correspondence and reprint requests to: C.C. van Donkelaar, Department of Biomedical Engineering, Gem-Z 4.101, Eindhoven University of Technology, PO Box 513, 5600 MB Eindhoven, The Netherlands. Tel: 31-40-247-3135.
E-mail addresses: s.m.hosseini@tue.nl (S.M. Hosseini), w.wilson@tue.nl (W. Wilson), k.ito@tue.nl (K. Ito), c.c.v.donkelaar@tue.nl (C.C. van Donkelaar).

1063-4584/$ – see front matter © 2013 Osteoarthritis Research Society International. Published by Elsevier Ltd. All rights reserved.
http://dx.doi.org/10.1016/j.joca.2013.10.010

cartilage damage is unknown. Various mechanisms can be postulated. Softening of the ground substance may reduce the compressive properties of the cartilage and this may subsequently put the collagen network at risk of overstraining. Alternatively, softening of the collagen network may allow the ground substance to attract more water, resulting in local tissue swelling. This may further weaken the tissue, which could result in excessive straining during mechanical loading. Indeed, OA was found to develop in animals that were treated with either collagenases or stromelysins[19,20], indicating that both PGs and collagen are essential to joint homeostasis. Yet, these studies did not reveal the mechanism by which softening of the PGs and collagen network may interact, and effects not related to tissue mechanics such as inflammation, may have played a role.

Therefore, the importance of softening in the ground substance, damage to the collagen network, and the possible interaction between these two for the progression of cartilage damage remains speculative. Yet, such insight may be useful for future development of therapies to treat early OA. To explore these effects experimentally is challenging. Therefore, a numerical approach is adopted, using a composition based model that includes collagen fiber-reinforcement, ground substance stiffness and tissue swelling due to PGs, and constitutes a physiological organization of the collagen structure and a depth dependent collagen and PG density[21,22]. To study progression of cartilage damage with this model requires extension, such that softening of the collagen network and of the ground substance may progress independently over time as a result of mechanical conditions in the tissue.

The objective of the present study is to present such damage progression model, and to employ it to explore whether and how damage in the PG-rich ground substance may advance damage in the collagen network and vice versa. For this purpose, simulations are compared in which cartilage is excessively loaded under four hypothetical conditions. The first condition is when no damage is allowed to develop in the cartilage as a reference. Second, damage is only allowed to develop in the fibrillar network. Third, damage only develops in the ground substance. Fourth, damage may develop in both the fiber network and the ground substance.

Materials and methods

Cartilage mechanics model

A composition-based, fiber-reinforced, poroviscoelastic biphasic swelling model is adopted[21,23,24], in which cartilage is assumed to consist of a porous solid matrix saturated with water. The solid consists of a PG-rich ground substance and a fibrillar part representing the collagen network. The ground substance has a particular stiffness and contains fixed negative charges associated with the PGs, which induce osmotic swelling. The viscoelastic fibrillar network is implemented in 2D as a collection of two primary and four secondary fiber directions per integration point. The primary fiber directions are oriented such that they represent the arcade-like organization and bend in opposite directions close to the surface. A less dense network of random fibrils in the tissue is represented by the four secondary fibers compartments, which run in vertical, horizontal and two oblique directions. The relative density of the primary fibers has previously been determined to be 3.009 times that of the secondary fiber directions, and has been taken into account in the collagen density ρ_c^i per fiber direction i (Eq. (1))[23]. The total stress ($\boldsymbol{\sigma}_{tot}$) in the cartilage is then determined by the combination of hydrostatic, non-fibrillar and fibrillar matrix stresses and osmotic pressure ($\Delta\pi$) (Eq. (1)).

$$\boldsymbol{\sigma}_{tot} = -p\mathbf{I} + n_{s,0}\left(\left(1-\sum_{i=1}^{totf}\rho_c^i\right)\boldsymbol{\sigma}_{nf} + \sum_{i=1}^{totf}\rho_c^i\boldsymbol{\sigma}_f^i\right) - \Delta\pi\mathbf{I} \tag{1}$$

where p is the hydrostatic pressure, $\mathbf{I}$ is the unit tensor, $n_{s,0}$ is the initial solid volume fraction, $\boldsymbol{\sigma}_{nf}$ is the Cauchy stress in the non-fibrillar matrix, σ_f^i is the fiber Cauchy stress in the ith fiber with respect to the global coordinate system, ρ_c^i is the volume fraction of the collagen fibers in the ith direction with respect to the total volume of the solid matrix and $\Delta\pi$ is the osmotic pressure gradient. The non-fibrillar and fibrillar stress terms are defined per unit area of the non-fibrillar and fibrillar areas respectively.

The non-fibrillar matrix stress can be calculated by the following formula, which depends on the amount of deformation, the amount of solid and shear modulus G_m[21,23]:

$$\boldsymbol{\sigma}_{nf} = -\frac{1}{6}\frac{\ln(J)}{J}G_m\mathbf{I}\left[-1+\frac{3(J+n_{s,0})}{(-J+n_{s,0})}+\frac{3\ln(J)Jn_{s,0}}{(-J+n_{s,0})^2}\right] + \frac{G_m}{J}\left(\mathbf{F}\cdot\mathbf{F}^T - J^{2/3}\mathbf{I}\right) \tag{2}$$

where J is the determinant of the deformation tensor $\boldsymbol{F}$.

The fiber Cauchy stress tensor is as follows:

$$\boldsymbol{\sigma}_f = \frac{\lambda}{J}P_f\vec{e}_f\vec{e}_f \tag{3}$$

where λ is the elongation of the fiber, P_f is the first Piola–Kirchhoff stress, and e_f is the current fiber direction. The total Cauchy stress of the fibers is expressed as a function of the deformed surface that a fiber works on. The viscoelastic behavior of the collagen fiber was represented by the two-parameter exponential stress–strain relationship springs S_1, parallel to a spring S_2 in series with a linear dashpot with dashpot constant η. The strain dependent stresses P_1 and P_2 in springs S_1 and S_2 are calculated as:

$$\begin{aligned} P_1 &= E_1\left(e^{k_1\varepsilon_f}-1\right) \quad \text{for } \varepsilon_f > 0 \\ P_2 &= E_2\left(e^{k_2\varepsilon_e}-1\right) = \eta\dot{\varepsilon_v} \quad \text{for } \varepsilon_e > 0 \end{aligned} \tag{4}$$

with E_1, E_2, k_1 and k_2 positive material constants, ε_f the total fiber strain, ε_e the strain in spring S_2 and ε_v the dashpot strain. Fibers are assumed to withstand tension (positive strains), but not compression. The total fiber stress P_f is the summation of P_1 and P_2[23].

The values of the model parameters used are[23]: $E_1 = 4.316$ MPa, $E_2 = 19.97$ MPa, $k_1 = 16.85$, $k_2 = 41.49$, $\eta = 1.424 \times 10^5$ MPa s, $G_m = 0.903$ MPa.

For formulations of the osmotic pressure and strain dependent permeability the reader is referred to Wilson *et al.*[23].

Damage model

The mechanics model is extended with a description of damage. Basically, it is assumed that when the deviatoric strain value in the ground substance exceeds a particular threshold, this would soften the matrix. For the fiber network, it is assumed that when the strain in the direction of the fibers exceeds a threshold, these fibers soften. As there may be a distribution of strains in the ground substance or in the collagen fibers, softening accumulates over time when during subsequent cycles a larger portion of the ground substance or fibers become damaged.

This theory is implemented using a damage parameter D, which represents the relative amount of damaged material and has a value

between 0 and 1. The effective stress for either the non-fibrillar or the fibrillar matrix then becomes:

$$\tilde{\boldsymbol{\sigma}} = \frac{\boldsymbol{\sigma}}{1-D} \tag{5}$$

The damage parameter D can be expressed as a function of a history variable κ_z, which equals the maximal value of the equivalent strain over time. The damage evolution law for D in the present study is defined similar for the fibrillar and the non-fibrillar matrix as:

$$D = \begin{cases} 0 & \text{if } \kappa_z \le \kappa_{0,z} \\ \frac{\kappa_{c,z}}{\kappa_z}\frac{\kappa_z-\kappa_{0,z}}{\kappa_{c,z}-\kappa_{0,z}} & \text{if } \kappa_{0,z} < \kappa_z < \kappa_{c,z} \\ 1 & \text{if } \kappa_z \ge \kappa_z \end{cases} \tag{6}$$

where $\kappa_{0,z}$ is the value of κ_z at which damage starts, and $\kappa_{c,z}$ is the value of κ_z at which the total tissue is damaged ($z = \{f, nf\}$ for the fibrillar (f) and non-fibrillar part (nf)).

For the equivalent strain (ε_{eq}) in the collagen fibers the strain in the direction of the collagen fibers was used:

$$\varepsilon_{eq,f}(\vec{x}) = \varepsilon_f(\vec{x}) \tag{7}$$

and for the non-fibrillar matrix the deviatoric strain equals:

$$\varepsilon_{eq,nf}(\vec{x}) = \frac{1}{3}\sqrt{\left(\varepsilon_{p1}(\vec{x})-\varepsilon_{p2}(\vec{x})\right)^2+\left(\varepsilon_{p1}(\vec{x})-\varepsilon_{p3}(\vec{x})\right)^2+\left(\varepsilon_{p2}(\vec{x})-\varepsilon_{p3}(\vec{x})\right)^2} \tag{8}$$

where ε_{pi} are the principal strains.

In a uniaxial stress situation, and assuming that the equivalent strain equals the axial strain, Eq. (6) results in linear softening, followed by complete loss of stiffness at $\kappa_{c,z}$ [Fig. 1].

Damage thresholds for the fibrillar and non-fibrillar matrix are based on data from the literature[25–29], but it should be noted that these data vary largely in the literature, as is extensively deliberated in the discussion. Fibrillar damage is assumed to start at 8% strain, while fibers are assumed to fail completely at 18% strain in the fiber direction ($\kappa_{0,f} = 0.08$; $\kappa_{c,f} = 0.18$). For the non-fibrillar matrix, it is assumed that complete failure of the non-fibrillar matrix would occur at 60% strain and that damage would start to initiate at half that strain level ($\kappa_{0,nf} = 0.30$; $\kappa_{c,nf} = 0.60$).

Simulations

A 2D model of articular cartilage (5.5 mm wide, 1 mm high; 1950 pore pressure plane strain elements with 4-node bilinear displacement CPE4P) was loaded with a round-end impermeable indenter (1 mm diameter)[Fig. 2] in ABAQUS 6.10 (Abaqus Inc., Providence, RI). The bottom is fixed in all directions to represent cartilage attachment to bone. Water is free to leave the tissue from the sides and top of the sample in which there is no contact with the indenter. The spatial distribution of PG and collagen, and the orientation of collagen are taken from the literature[21,23].

First, the tissue was allowed to equilibrate for 8 h in 0.15 M solution, during which the tissue swelled approximately 1%. Subsequently, the indenter compressed the tissue in four steps of 10% compression to 10, 20, 30 and 40% of the original tissue height at a strain rate of 0.1% s^{-1}. Each loading step was followed by 2 h of stress-relaxation.

This protocol is simulated for four different conditions. First, a control case in which no damage was allowed to develop in the cartilage ('No damage'). Second, damage was only permitted to develop in the fibers ('Fiber damage only'). Third, damage was only permitted to develop in the ground substance ('Ground substance damage only'). Fourth, damage was permitted to develop in both the fibers and the ground substance ('Both fiber and ground substance damage'). Fiber damage is computed at each location for each of the two primary and four secondary fibers in the six directions. The total normalized fiber network damage per location is then calculated as the average damage in all fibers, weighted for their respective densities (Eq. (9)):

$$D_{\text{Fibrillar Network}} = \frac{C(D_{P1}+D_{P2})+D_{S1}+D_{S2}+D_{S3}+D_{S4}}{2C+4} \tag{9}$$

where D_P and D_S are the damage parameter in each primary and secondary fiber direction respectively and $C = 3.009$ is the relative density of the primary fibers with respect to the secondary fibers[23], as accounted for in the collagen density parameter in Eq (1).

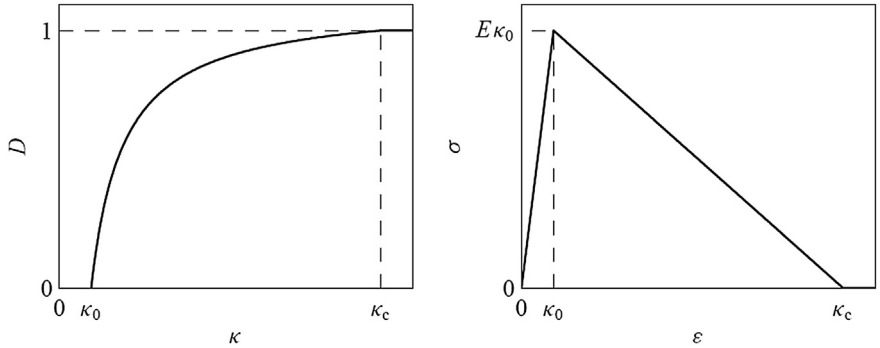

Fig. 1. Damage model, showing the damage variable (D) as a function of the strain history variable (κ, ranging from κ_0 to κ_c) (left) and the corresponding softening of the constituent, visualized by the stress-strain behavior of the tissue (right).

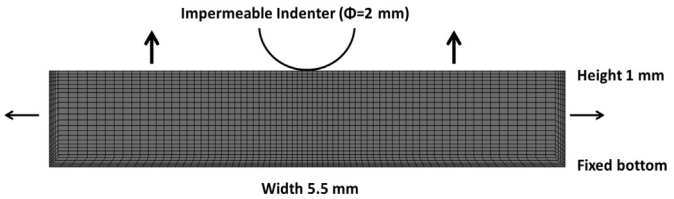

Fig. 2. 2D finite element mesh of the cartilage sample and the indenter. The bottom is fixed to simulate attachment to the bone. Arrows indicate free surfaces with unrestricted water flow.

Results

As the loading increased, damage developed in both the fibrillar network and ground substance. The area where damage occurred was different for the two components [Fig. 3(a)–(d)]. These locations remained largely the same, regardless of whether damage occurred in only one of the components [Fig. 3(a),(c)] or in both [Fig. 3(b),(d)], but if both were allowed to occur, the ground substance damage penetrated deeper and fiber network damage was enhanced [Fig. 3(e)].

To obtain a better insight in the damage development, ground substance and fiber matrix damage were evaluated separately and as a function of the depth of indentation. Ground substance softening started at the surface and gradually developed deeper into the tissue [Fig. 4(a)]. Maximal damage remained located at the surface, and there was a steep transition from highly damaged areas to deeper undamaged regions. Initial superficial damage started already at 10% indentation loading, because even at this low external indentation, due to the round shape of the indenter the local strains inside the tissue exceeded 30%.

Damage in the fiber network started in the transition zone, i.e., in the area underneath the surface, while the superficial zone remained intact [Fig. 4(b)]. When the indentation depth reached higher strain levels, damage penetrated into the deeper areas of the cartilage, while more intense damage occurred in the superficial zone [Fig. 4(b)].

The magnitude and location of fiber damage depended on the orientation of the fibers. For fibers parallel to the surface, which are part of the pool of secondary fibers, the damage was more severe than for perpendicular or oblique fibers [Fig. 5]. Secondary fibers show more intense damage underneath the surface, while primary fibers are damaged in the superficial zone after more severe loading [Fig. 4]. Due to the lower volume fraction of the secondary fibers their effect on the total stress might be less than the effect of the damage in the primary fibers. The fibers in vertical direction did not damage because they did not undergo tension during the applied loading protocol, while oblique fibers did not damage because the strain in their direction did not exceed the threshold ($\kappa_{0,f} = 0.08$) (data not shown).

Compared with undamaged cartilage, the peak force and the equilibrium relaxation force decreased when damage developed in the tissue [Fig. 6]. The magnitude of these changes depended on the nature of damage, with ground substance softening reducing the stiffness more than fiber damage.

Finally, the local damage in the tissue not only changed the local effective stress, but also the distribution of strains inside the tissue, as illustrated by maximum principal strain at the end of the 40% indentation [Fig. 7]. Compared with the strain distribution in

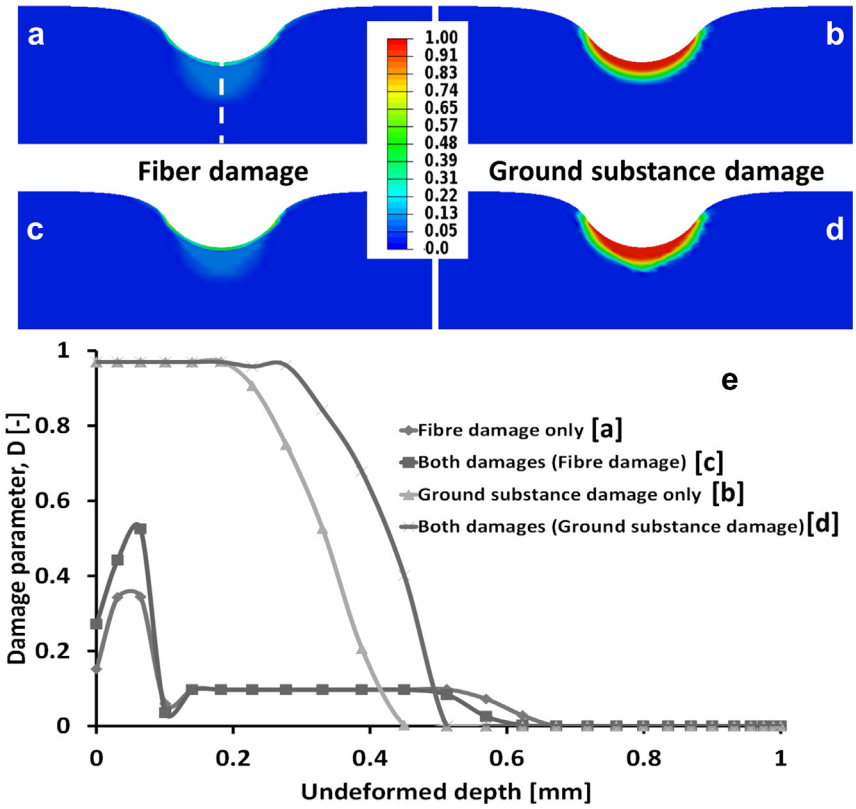

Fig. 3. Damage distribution in the fibers (a,c) and the ground substance (b,d) at the end of the loading protocol when only fiber damage (a), only ground substance damage (b), or both are allowed to occur in parallel (c,d). Colors represent the magnitude of damage parameter *D*, which is quantitatively shown in (e) as a function of depth from the surface (0 mm) to the bone (1 mm) over an imaginary line centrally under the indenter (indicated as a dash white line in (a)).

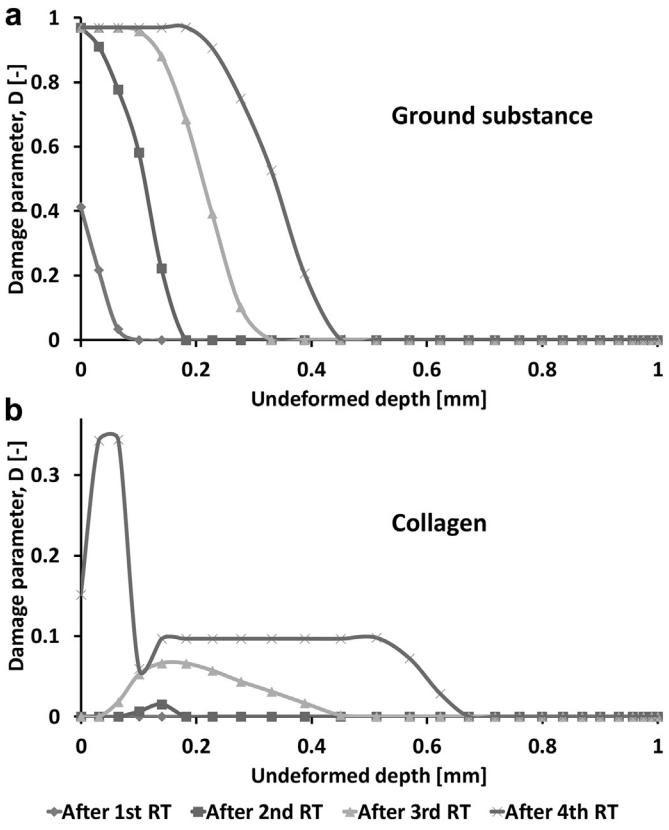

Fig. 4. The profile of damage at the end of the stress-relaxation period following each of the four subsequent loading cycles shows progression of the damage over time. The horizontal axis represents an imaginary line centrally under the indenter from the surface (0 mm) to the bone (1 mm), similar to Fig. 3(e). Top: damage in the ground substance; bottom: damage in the collagen fiber network.

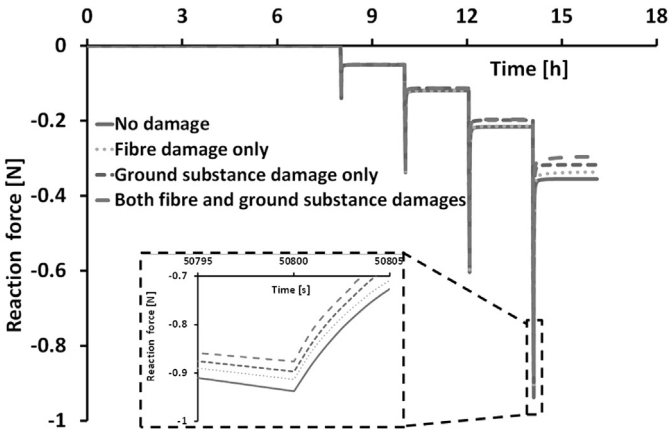

Fig. 6. Reaction force during the four simulations over time, where strain was increased to 10, 20, 30 and 40% after 8, 10, 12 and 14 h, respectively. A magnification is included of the peak values after 40% strain was applied.

undamaged tissue [Fig. 7(a)], the distribution of strains was less affected by softening of the ground substance [Fig. 7(c)] than by damage in the fibers [Fig. 7(b),(d)]. When both damages are present, the effect on strain was most distinctive, with sharp transition areas centrally under the surface [Fig. 7(d)].

Discussion

A damage progression model for articular cartilage is presented, based on an established composition-based model for cartilage mechanics. It can independently predict the development of softening in the ground substance and damage in the fibrillar network over time and as a function of mechanical loading. The model is employed to evaluate theoretical effects of ground substance softening and collagen damage on tissue softening, and to explore whether damage in the ground substance may advance damage in the collagen network and vice versa. Ground substance softening is predicted to develop over a larger area than collagen damage under the applied indentation loading [Fig. 3]. Cartilage softening, an important measure for cartilage function, is affected earlier and to a greater extent by damage in the ground substance than by collagen damage. Softening due to ground substance damage is promoted by additional collagen damage [Fig. 6]. Collagen damage has a more pronounced effect on the magnitude and distribution of strains inside the tissue, and this effect is more prominent when the ground substance is allowed to soften simultaneously [Fig. 7]. The concentration of high strains and the strain gradients that develop underneath the surface in the transitional zone [Fig. 7 (b),(d)] seem unfavorable and may be speculated to be detrimental to the cartilage in the long-term, possibly also via effects on chondrocyte viability, which was shown to decrease with the development of damage in overloaded cartilage[30,31]. Summarized, the simulations suggest that ground substance softening is more essential to cartilage softening, while damage to the collagen induces an unfavorable strain field in the tissue. Additionally, due to mechanical interaction between the ground substance and the collagen fibers, damage to either one of them can promote damage in the other. Alternatively formulated, the results suggest that if the components are intact, they protect each other from developing damage.

The above conclusions, however, need to be considered with care. They depend on the validity of the model, and the presented model has not yet been validated thoroughly against experimental data. It is an extension of a validated composition based model for cartilage, which includes reinforcement with a viscoelastic fiber

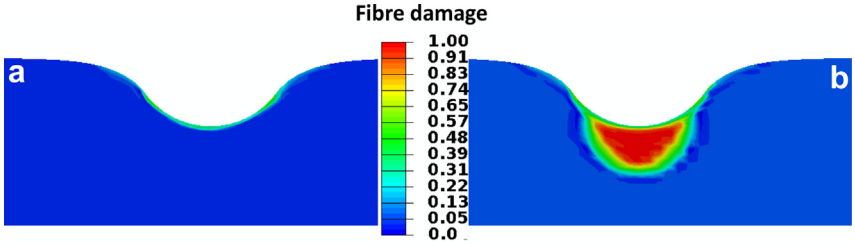

Fig. 5. Damage in the fibrillar network was dependent on the fiber orientation, as shown here for the simulation in which fiber damage was only allowed to occur. a: Damage in one of the primary fibers with an arcade-like orientation. b: Damage in the secondary fiber compartment that has a horizontal orientation. Results belong to the end of the loading protocol.

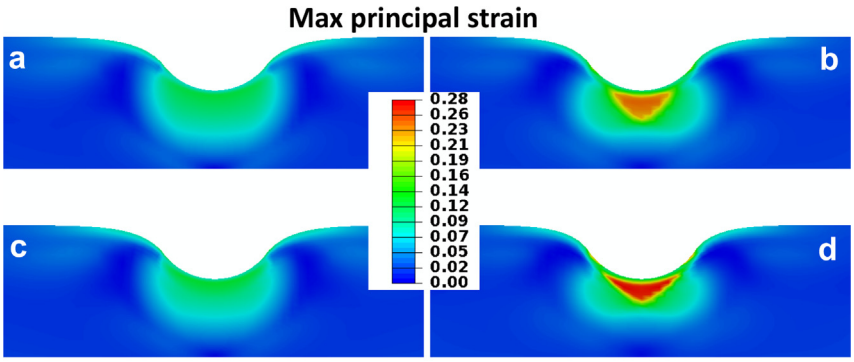

Fig. 7. Maximum principal strain distributions, 2 h after 40% indentation was applied, in case no damage was allowed to develop (a), or damage developed in the fibers (b), the ground substance (c) or both (d).

network, and biphasic swelling. The biphasic swelling approach was analytically validated for swelling values in the physiological range of cartilage[21], and material parameters for swelling, non-fibrillar matrix and the fiber network have been fitted simultaneously to unconfined and confined compression, indentation and free swelling data from the literature[23,32]. Subsequently, the model has proven to be valuable to understand several aspects of cartilage mechanics, enforcing the validity of this approach. However, the damage model that is now added has not yet been validated for cartilage. The description using a damage parameter and a strain history variable is common in polymer science[33], and the relationship between these parameters that was employed here (Eq. (6)) is the simplest version of this approach. Although a more difficult damage law may turn out to apply for cartilage in the future, variations are not anticipated to change the general conclusions. The most important and critical unknown factors are the four values that were chosen as damage thresholds ($\kappa_{0,f}$, $\kappa_{c,f}$, $\kappa_{0,nf}$, and $\kappa_{c,nf}$ (Eq. (6); Fig. 1)). The exact values for these thresholds, which represent damage in a continuum that contains a number of fibers that may experience different strain magnitudes, are unknown. The values that are used have been estimated from experiments on articular cartilage, on collagen-rich tissues, and on individual fibers under various loading conditions[25–29,34–38]. Failure strain measurements for collagen type II have not been reported. From an inversed analysis, collagen failure strains inside cartilage were estimated to be as high as 28%[13], but this actual value was mentioned to be taken with caution. This is in the same order of magnitude as the yield (20%) and failure strain (30–50%) previously reported for individual collagen fibrils[28]. Also, failure strain of the collagen-rich superficial zone cartilage were reported in the order of 25–40%[37,38], and this concurs with Huang *et al.*[34] who neither observed failure in a tensile test of articular cartilage till 16% strain, nor in confined compression till 50% strain. An extensive review on tendons[27], however, reported microscopic damage of collagen type I to start beyond 4% strain, with more severe damage occurring when strains reached 8–10%[35], whereas human patellar tendons only fail at strains in the order of 14–16%. Failure of self-assembled collagen fibers that were cross-linked at either zero or 50% stretch failed at 15.59% or 11.65% strain, respectively[36]. Taken together, it is assumed that fibrillar damage starts at 8% strain and that damage is complete at 18% strain in the fiber direction ($\kappa_{0,f} = 0.08$; $\kappa_{c,f} = 0.18$). Data on strains that induce damage to the ground substance are not known. It is assumed that the ground substance is much more compliant than the collagen fibrils. For adult bovine cartilage, complete failure strains were reported in the order of 60%[25], at which also the more compliant part of the tissue failed. Another study mentioned failure strain for cartilage to be 30%, but without appropriate reference[29]. Therefore, it is assumed that complete failure of the non-fibrillar matrix would occur at 60% strain and that damage would start to initiate at half that strain level ($\kappa_{0,nf} = 0.30$; $\kappa_{c,nf} = 0.60$).

To evaluate the effect of the chosen parameter values for $\kappa_{0,z}$ and $\kappa_{c,z}$, a simple parameter variation study was performed. Although the size of the affected area and the magnitude of damage depend on these values, the locations of damage, the patterns of damage progression over time, and the nature of the interaction between damage in the ground substance and the collagen fibers are insensitive to these parameters. This insensitivity is also illustrated by noting that damage initiates earlier and progresses more rapidly in the ground substance than in the fibers [Fig. 6], even though $\kappa_{0,nf}$ for the ground substance is three times larger than $\kappa_{0,f}$ for the fibrillar network.

Although full validation of the damage model has not yet been performed, the output may be compared with literature data to evaluate the predictions. Reduction in mechanical properties over time with progression of tissue damage [Fig. 6] is known to occur experimentally and clinically[11,14,37,39–42]. In agreement with the present findings (combine Figs. 4 and 6), it has been shown that cartilage softening after indentation already occurs before collagen damage can be observed[14]. Also, the prediction that compromised ground substance may affect the failure mechanics of collagen and vice versa was previously observed, although this involved tensile testing and not compression[37]. The regions in which damage is predicted to occur are probably the best data for validation. The location of predicted ground substance damage matches with experimental and clinical observations of PG loss[13,30,31,43–46]. Loss of safranin-O staining starts at the articular surface[30,31,43,47] and this area increases with increased loading, while a sharp transition remains between the PG-rich and the PG-poor tissue[43]. This concurs with the predictions [Figs. 3(b),(d),(e) and 4]. It should be noted that PG loss was not incorporated as such in the model. Ground substance weakening was assumed to occur, but the fixed charge density remained constant. However, it makes sense that damaging of the ground substance precedes the loss of PGs. The rationale is that excessive straining may fracture the PGs into smaller fragments, which would subsequently be able to diffuse out of the tissue into the synovial fluid. However, it was shown that such loss may take up to 48 h[47] which may explain why no loss of PGs was seen immediately after damage was induced by indentation[24].

Collagen damage also increases with tissue loading. Intense staining for collagen damage is found selectively in the superficial zone of human OA cartilage, while more diffuse collagen damage penetrates deeper into the tissue over a larger area[43]. It has been

shown that the deeper and diffuse collagen damage may precede the more intense damage in the superficial zone when excessive indentation is applied[13]. Also, collagen already exhibits impaired load bearing properties already in very early OA tissue[48]. All these data suggest that the collagen network may be mechanically compromised in the transitional or deeper zone before visible damage such as fissures become apparent at the surface. This is in agreement with the present predictions. Finally, Fig. 7 shows significant changes in the internal strain field in the cartilage. This is in agreement with textural histological alterations seen in the superficial cartilage after applied tissue injury[47], as well as with significant changes in tissue deformation found between explants that were loaded in the presence or absence of a superficial tangential zone[24,49]. Interestingly, the peculiar triangular pattern of strains and the sharp transition between high and low strained areas in the tissue corresponds with recent publications on internal collagen deformation patterns in severely loaded articular cartilage as observed with DIC[49]. Even though the loading protocol that was used in the latter study was different (single vs double indenter) it may be speculated that the strains penetrated similarly into the tissue. In a previous numerical study using the same composition based model employed here[24], yet without damage, the global strain patterns of the experiments by Bevill *et al.*[49] were corroborated. However, the sharp transitions were not seen in the model, which may now be speculated to be caused by initial collagen damage in the experiments, which was not accounted for in former simulations[24].

Some limitations require discussion. Although the results were independent of the mesh size that was used, mesh-dependent localization of damage is an issue in damage mechanics. This could theoretically be solved by using nonlocal or enhanced gradient methods for the damage evolution[50,51], which may be required for answering questions related to the propagation of fissures. Also, 3D rather than 2D modeling may be required for particular future studies. However, this is not essential for the first assessment of the interaction between ground substance softening and collagen damage, which is the objective of the present study. Finally, the present simulations addressed collagen and PG damage in a 1 mm thick cartilage that was mechanically loaded with a 1 mm diameter indenter at a loading rate of 0.1% s^{-1}. These conditions were chosen as they were known to induce collagen damage[13] and could therefore serve to study the behavior of the model under damaging loading conditions. Yet, the chosen conditions themselves have limited clinical relevance. The shape of the indenter does not represent the shape of joint and collagen damage is known to be more pronounced at higher loading rates, i.e., under impact loading[30,31]. Although this is beyond the scope of the present study, the effects of indenter geometry, dynamic vs static loading, and cartilage thickness will be evaluated in future studies in which the model will further be validated.

After thorough validation of damage prediction in explants under controlled experimental conditions has been performed, the next steps in this research will be two fold. First, the geometry will be extended to realistic 3D joint surfaces. Second, a biological repair response will be implemented, adopting an already developed numerical approach[52]. Ultimately, mechanically induced damage progression, biological repair responses and realistic geometries based on clinical MR images could together provide a means to make a patient specific prognosis of the progression of OA.

Conclusion

A cartilage damage progression model is proposed and employed to explore effects of ground substance softening and collagen fiber damage on cartilage mechanopathology. Even though thorough validation is still required, predictions of the locations and magnitudes of damage in both constituents, and the effects thereof on cartilage softening and tissue strain corroborate well with the literature.

Based on the results, it is concluded that damage to the ground substance has more pronounced effects on cartilage softening, while damage to the collagen network results in adverse strain localizations inside the tissue. Importantly, it is shown that damage to either one of them can promote damage in the other, while an intact collagen network may protect the ground substance from softening and vice versa.

Contributions

All authors contributed to the conception and design of the study, analysis and interpretation of the data. S.M. Hosseini performed the final simulations and experiments, and drafted the article. All authors contributed to the revision of the article and granted final approval.

Competing interests

All authors declare to have no competing interests.

Role of the funding source

This project has been funded by the Dutch Arthritis Foundation, which did not have a role in the study design, collection, analysis and interpretation of data, nor in the writing of the manuscript and the decision to submit the manuscript for publication.

References

1. Thibault M, Robin Poole A, Buschmann MD. Cyclic compression of cartilage/bone explants in vitro leads to physical softening, mechanical breakdown of collagen and release of matrix fragments. J Orthopaedic Res 2002;20:1265–73.
2. Jeffrey JE, Anne Thomson L, Aspden RM. Matrix loss and synthesis following a single impact load on articular cartilage in vitro. Biochim Biophys Acta 1997;1334(2–3):223–32.
3. Jeffrey JE, Gregory DW, Aspden RM. Matrix damage and chondrocyte viability following a single impact load on articular cartilage. Arch Biochem Biophys 1995;322(1):87–96.
4. Anderson DD, Chubinskaya S, Guilak F, Martin JA, Oegema TR, Olson SA, *et al.* Post-traumatic osteoarthritis: improved understanding and opportunities for early intervention. J Orthopaedic Res 2011;29(6):802–9.
5. Chen MH, Broom N. On the ultrastructure of softened cartilage: a possible model for structural transformation. J Anat 1998;192:329–41.
6. Radin EL, Ehrlich MG, Chernack R, Abernethy P, Paul IL, Rose RM. Effect of repetitive impulsive loading on the knee joints of rabbits. Clin Orthop 1978;131:288–93.
7. Pelletier JP, Martel-Palletier J, Altman RD, Ghandur-Mnaymneh L, Hower DS, Woessner JF. Collagenolytic activity and collagen matric breakdown of the articular cartilage in de Pond-Nuki dog model of osteoarthritis. Arthritis Rheum 1983;26:866–74.
8. Guilak F, Ratcliffe A, Lane N, Rosenwasser MP, Mow VC. Mechanical and biochemical changes in the superficial zone of articular cartilage in canine experimental osteoarthritis. J Orthop Res 1994;12:474–84.
9. Clark JM, Simonian PT. Scanning electron microscopy of 'fibrillated' and 'malacic' human articular cartilage: technical considerations. Microsc Res Techn 1997;37:299–313.
10. Akizuki S, Mow VC, Müller F, Pita JC, Howell DS, Manicourt DH. Tensile properties of human knee joint cartilage: I. Influence of

ionic conditions, weight bearing and fibrillation on the tensile modelus. J Orthop Res 1986;4:379–92.
11. McCormack T, Mansour JM. Reduction in tensile strength of cartilage precedes surface damage under repeated compressive loading in vitro. J Biomech 1998;31:55–61.
12. LeRoux MA, Setton LA. Experimental and biphasic FEM determinations of the material properties and hydraulic permeability of the meniscus in tension. ASME J Biomech Eng 2002;124:315–21.
13. Wilson W, van Burken C, van Donkelaar CC, Buma P, van Rietbergen B, Huiskes R. Causes of mechanically induced collagen damage in articular cartilage. J Orthop Res 2006;24:220–8.
14. Hosseini SM, Veldink MB, Ito K, van Donkelaar CC. Is collagen fiber damage the cause of early softening in articular cartilage? Osteoarthritis Cartilage 2013;21(1):136–43.
15. Chen MH, Broom ND. Concerning the ultrastructural origin of large-scale swelling in articular cartilage. J Anat 1999;194(Pt 3):445–61.
16. Broom N, Chen MH, Hardy A. A degeneration-based hypothesis for interpreting fibrillar changes in the osteoarthritic cartilage matrix. J Anat 2001;199(Pt 6):683–98.
17. Elliot DM, Guilak F, Vail TP, Wang JY, Setton LA. Tensile properties of articular cartilage are altered by meniscectomy in a canine model of osteoarthritis. J Orthopaed Res 2000;18(3):383–92.
18. Thambyah A, Broom N. On how degeneration influences load-bearing in the cartilage–bone system: a microstructural and micromechanical study. Osteoarthritis Cartilage 2007;15(12):1410–23.
19. Tesch AM, MacDonald MH, Kollias-Baker C, Benton HP. Endogenously produced adenosine regulates articular cartilage matrix homeostasis: enzymatic depletion of adenosine stimulates matrix degradation. Osteoarthritis Cartilage 2004;12(5):349–59.
20. Eyre DR. Collagens and cartilage matrix homeostasis. Clin Orthop Relat Res 2004;427:118–22.
21. Wilson W, Huyghe JM, von Donkelaar CC. Depth dependent compressive equilibrium properties of articular cartilage explained by its composition. Biomech Model Mechanobiology 2007;6:43–53.
22. Julkunen P, Wilson W, Jurvelin JS, Rieppo J, Qu CJ, Lammi MJ, *et al*. Stress–relaxation of human patellar articular cartilage in unconfined compression: prediction of mechanical response by tissue composition and structure. J Biomech 2008;41(9):1978–86.
23. Wilson W, Huyghe JM, van Donkelaar CC. A composition-based cartilage model for the assessment of compositional changes during cartilage damage and adaptation. Osteoarthritis Cartilage 2006;14(6):554–60.
24. Hosseini SM, Wu Y, Ito K, van Donkelaar CC. The importance of superficial collagen fibrils for the function of articular cartilage. Biomech Model Mechanobiol. in press, http://dx.doi.org/10.1007/s10237-013-0485-0;.
25. Williamson AK, Chen AC, Masuda K, Thonar EJ, Sah RL. Tensile mechanical properties of bovine articular cartilage: variations with growth and relationships to collagen network components. J Orthopaedic Res 2003;21:872–80.
26. Haut RC. The influence of specimen length on the tensile failure properties of tendon collagen. J Biomechanics 1986;19(11):951–5.
27. Wang JH-C. Review mechanobiology of tendon. J Biomech 2006;39:1563–82.
28. Shen ZL, Dodge MR, Kahn H, Ballarini R, Eppell SJ. Stress-strain experiments on individual collagen fibrils. Biophys J 2008;95:3956–63.
29. Stammen JA, Williams S, Ku DN, Guldberg RE. Mechanical properties of a novel PVA hydrogel in shear and unconfined compression. Biomaterials 2001;22:799–806.
30. Chen CT, Bhargava M, Lin PM, Torzilli PA. Time, stress, and location dependent chondrocyte death and collagen damage in cyclically loaded articular cartilage. J Orthop Res 2003;21(5):888–98.
31. Ewers BJ, Dvoracek-Driksna D, Orth MW, Haut RC. The extent of matrix damage and chondrocyte death in mechanically traumatized articular cartilage explants depends on rate of loading. J Orthop Res 2001;19(5):779–84.
32. Wilson W, van Donkelaar CC, van Rietbergen B, Huiskes R. A fibril-reinforced poroviscoelastic swelling (FPVES) model for articular cartilage. J Biomech 2005;38:1195–204.
33. Geers MGD, de Borst R, Brekelmans WAM, Peerlings RHJ. Validation and internal length scale determination for a gradient damage model: application to short glass-fiber-reinforced polypropylene. Int J Sol Structures 1999;36(17):2557–83.
34. Huang C-Y, Stankiewicz A, Ateshian GA, Mow VC. Anisotropy, inhomogeneity, and tension–compression nonlinearity of human glenohumeral cartilage in finite deformation. J Biomech 2005;38:799–809.
35. Butler DL, Grood ES, Noyes FR, Zernicke RF. Biomechanics of igaments and tendons. Exerc Sport Sci Rev 1978;6:125–81.
36. Pins GD, Huang EK, Christiansen DL, Silver FH. Effects of static axial strain on the tensile properties and failure mechanisms of self-assembled collagen fibers. J Appl Polym Sci 1997;63:1429–40.
37. Kempson GE, Muir H, Pollard C, Tuke M. The tensile properties of the cartilage of human femoral condyles related to the content of collagen and glycosaminoglycans. Biochem Biophys Acta 1973;297:465–72.
38. Roth V, Mow VC. The intrinsic tensile behavior of the matrix of bovine articular cartilage and its variation with age. J Bone Joint Surg Am 1980;62:1102–17.
39. Temple MM, Bae WC, Chen MQ, Lotz M, Amiel D, Coutts RD, *et al*. Age- and site-associated biomechanical softening of human articular cartilage of the femoral condyle. Osteoartjritis Cartilage 2007;15(9):1042–52.
40. Buckwalter JA, Mow VC, Ratcliffe A. Restoration of injured or degenerated articular cartilage. J Am Acad Orthop Surg 1994;2(4):192–201.
41. Langelier E, Buschmann MD. Increasing strain and strain rate strengthen transient stiffness but weaken the response to subsequent compression for articular cartilage in unconfined compression. J Biomech 2003;36:853–9.
42. Akizuki S, Mow VC, Muller F, Pita JC, Howell DS. Tensile properties of human knee joint cartilage. II. Correlations between weight bearing and tissue pathology and the kinetics of swelling. J Orthop Res 1987;5:173–86.
43. Lin PM, Chen C-TC, Torzilli PA. Increased stromelysin-1 (MMP-3), proteoglycan degradation (3B3- and 7D4) and collagen damage in cyclically load-injured articular cartilage. OsteoArthritis Cartilage 2004;12:485–96.
44. Wu W, Billinghurst RC, Pidoux I, Antoniou J, Zukor D, Tanzer M, *et al*. Sites of collagenase cleavage and denaturation of type II collagen in aging and osteoarthritic articular cartilage and their relationship to the distribution of matrix metalloproteinase 1 and matrix metalloproteinase 13. Arthritis Rheum 2002;46(8):2087–94.
45. Hollander AP, Pidoux I, Reiner A, Rorabeck C, Bourne R, Poole AR. Damage to type II collagen in aging and osteoarthritis starts at the articular surface, originates around chondrocytes, and extends into the cartilage with progressive degeneration. J Clin Invest 1995;96:2859–69.

46. Lorenz H, Richter W. Osteoarthritis: cellular and molecular changes in degenerating cartilage. Prog Histochem Cytochem 2006;40:135–63.
47. Rolauffs B, Muehleman C, Li J, Kurz B, Kuettner KE, Frank E, *et al*. Vulnerability of the superficial zone of immature articular cartilage to compressive injury. Arthritis Rheum 2010;62(10):3016–27.
48. Thambyah A, Zhao J-Y, Bevill SL, Broom ND. Macro-, micro- and ultrastructural investigation of how degeneration influences the response of cartilage to loading. J Mech Behav Biomed Mater 2012;5(1):206–15.
49. Bevill SL, Thambyah A, Broom ND. New insights into the role of the superficial tangential zone in influencing the microstructural response of articular cartilage to compression. Osteoarthritis Cartilage 2010;18:1310–8.
50. de Vree JHP, Brekelmans WAM, van Gils MAJ. Comparison of nonlocal approaches in continuum damage mechanics. Comput Struct 1995;55:581–8.
51. Peerlings RHJ, de Borst R, Brekelmans WAM, Geers MGD. Gradient-enhanced damage modelling of concrete fracture. Mech Cohes-Friction Mater 1998;3:323–42.
52. van Donkelaar CC, Wilson W. Mechanics of chondrocyte hypertrophy. Biomech Model Mechanobiology 2012;11(5):655–64.